Journal of Computational and Applied Mathematics 235 (2010) 615–630

Contents lists available at ScienceDirect

Journal of Computational and Applied Mathematics

journal homepage: www.elsevier.com/locate/cam

Legendre–Laguerre coupled spectral element methods for second- and fourth-order equations on the half line

Qingqu Zhuang [a], Chuanju Xu [b,*]

[a] School of Mathematical Sciences, Huaqiao University, 362021 Quanzhou, China
[b] School of Mathematical Sciences, Xiamen University, 361005 Xiamen, China

ARTICLE INFO

Article history:
Received 23 August 2009
Received in revised form 15 May 2010

Keywords:
Spectral element method
Laguerre function
Elliptic problem
Unbounded domain

ABSTRACT

Some Legendre spectral element/Laguerre spectral coupled methods are proposed to numerically solve second- and fourth-order equations on the half line. The proposed methods are based on splitting the infinite domain into two parts, then using the Legendre spectral element method in the finite subdomain and Laguerre method in the infinite subdomain. C^0 or C^1-continuity, according to the problem under consideration, is imposed to couple the two methods. Rigorous error analysis is carried out to establish the convergence of the method. More importantly, an efficient computational process is introduced to solve the discrete system. Several numerical examples are provided to confirm the theoretical results and the efficiency of the method.

1. Introduction

Many mathematical problems in science and engineering are set in unbounded domains. There is thus a need to consider practical design and implementation issues in scientific computing for reliable and efficient solutions of these problems. For problems set up in unbounded domains, the traditional way for their numerical solutions is to restrict calculations to some bounded subdomains together with certain imposed conditions on artificial boundaries, and then solve the corresponding approximate problems. The drawback of this strategy is that the boundary conditions are usually unknown, and the use of inexact artificial conditions will affect the accuracy of the numerical results. An alternative strategy for these problems is to work directly in unbounded domains, with design methods by using suitable approximation spaces. It is now becoming known that Laguerre polynomials are good candidates for the construction of such approximation spaces. In fact, there have been several works aimed at this interesting direction. For example, some methods using Laguerre polynomials/functions for problems on unbounded domains have been developed, see [1–5]. These methods take advantage of the Laguerre polynomials, which are orthogonal with respect to the weight function e^{-x} on the half line. Generally, the larger the degree of the Laguerre polynomials/functions used to approximate the solutions, the smaller the errors of numerical solutions. However, from a practical point of view, the fact that the distance between the adjacent Laguerre Gauss–Radau points increases very fast as the polynomial degree increases may lead to undesirable consequences. In particular, the numerical solution may fit the exact solution badly when the latter exhibits high frequency spectra. This means that using single Laguerre polynomials/functions in the whole domain is not efficient for practical computations.

To overcome this inefficiency, a stair Laguerre method was proposed in [6] for the model Helmholtz equation. The method consists of progressively using the Laguerre method within a series of subintervals. However this method seems to be unable to completely overcome the difficulty due to the non-equilibrium of the Laguerre node distribution. In [7],

* Corresponding author.
E-mail address: cjxu@xmu.edu.cn (C. Xu).

0377-0427/$ – see front matter © 2010 Elsevier B.V. All rights reserved.
doi:10.1016/j.cam.2010.06.013

a composite Laguerre–Legendre method was constructed for approximating elliptic problems in unbounded domains. As a generalization of the work [7], a Legendre spectral element/Laguerre coupled method was introduced and analyzed in [8] for the Helmholtz problem in unbounded domains. The method combines the good properties of the spectral element method with the advantage of the Laguerre method in dealing with unbounded domains, and thus is capable to provide a high accurate solution in any interested bounded subdomains.

In this paper we will follow the idea of [8], and furthermore consider Legendre spectral element/Laguerre spectral coupled methods for second- and fourth-order equations on the half line. As compared to our previous work, the contribution of the present paper is threefold: (1) We construct a coupled Legendre spectral element/Laguerre spectral method for second-order as well as fourth-order elliptic equations. (2) We give a detailed analysis of the proposed methods by providing some rigorous error estimates. Thanks to the use of the Laguerre functions instead of the Laguerre polynomials employed in [8], the function change made in [8] becomes unnecessary, and thus the error analysis is greatly simplified. Moreover, the generalization to the fourth-order problem becomes much more natural. (3) Finally, an efficient implementation technique is proposed to accelerate the computation process, together with some numerical validations.

The rest of the paper is organized as follows: In Section 2, a Legendre spectral element/Laguerre spectral coupled method is presented for the second order problem. Rigorous convergence analysis is carried out. An efficient implementation strategy using a carefully chosen modal basis is detailed. In Section 3, the coupled spectral method is generalized to the fourth-order problem, together with some error estimates. Some concluding remarks are given in Section 4.

2. Coupled spectral method for second-order equations

2.1. Problem and approximation

Let $R^+ = (0, +\infty)$ and α be a positive constant. We consider the following second-order problem:

$$\begin{cases} -\partial_x^2 u + \alpha u = f, \quad x \in R^+, \\ u(0) = 0, \qquad \lim_{x\to+\infty} u(x) = 0. \end{cases} \tag{2.1}$$

In order to define the weak problem, some basic notations are useful. Let I be a finite or infinite interval and ω be a positive function. We use $H^m_\omega(I)$ and $H^m_{0,\omega}(I),\ m \geq 0$, to denote the usual ω-weighted Sobolev spaces with norm $\|\cdot\|_{m;\omega,I}$. We denote by $(u, v)_\omega := \int_I uv\omega dx$ the inner product of $L^2_\omega(I)$ whose norm is denoted by $\|\cdot\|_{0;\omega,I}$. In cases where no confusion would arise, ω (if $\omega \equiv 1$) and I may be dropped from the notations.

The coupled spectral method to be introduced is based on decomposing the infinite domain R^+ into a set of subdomains, then using different kinds of methods in different subdomains. To this end, let $\Lambda = (0, a)$ and $R^+_a = (a, +\infty)$. The subdomain Λ is then further partitioned into K non-overlapping subdomains $\Lambda^k = (a_{k-1}, a_k),\ k = 1, 2, \ldots, K$, where $a_k,\ k = 0, 1, \ldots, K$, are $K + 1$ points such that $0 = a_0 < a_1 < \cdots < a_K = a$. Let $h_k = a_k - a_{k-1}$ and $h = \max_{1\leq k\leq K} h_k$.

We then define the piecewise polynomial space as follows:

$$\mathbb{P}_{N,K}(\Lambda) := \{v;\ v_{|\Lambda^k} \in \mathbb{P}_N(\Lambda^k),\ k = 1, 2, \ldots, K\},$$

where $\mathbb{P}_N$ denotes the space of all polynomials of degree less than or equal to N.

Let $\mathcal{L}_i(x)$ be the Laguerre polynomial of degree i and $\hat{\mathcal{L}}_i(x)$ be the Laguerre function defined by:

$$\hat{\mathcal{L}}_i(x) = \mathcal{L}_i(x)e^{-x/2}, \quad \forall x \in R^+.$$

We also define the spaces:

$$\mathbb{P}_M(R^+_a) = \text{span}\{\mathcal{L}_i(x - a),\ i = 0, 1, \ldots, M\},$$

and

$$\hat{\mathbb{P}}_M(R^+_a) = \text{span}\{\hat{\mathcal{L}}_i(x - a),\ i = 0, 1, \ldots, M\}.$$

Let $\mathcal{N}$ denote the set of discrete parameters (N, K, M). We define the global approximation spaces:

$$S_{\mathcal{N}} = \{v;\ v_{|\Lambda} \in \mathbb{P}_{N,K}(\Lambda),\ v_{|R^+_a} \in \hat{\mathbb{P}}_M(R^+_a)\},$$

$$X_{\mathcal{N}} = S_{\mathcal{N}} \cap H^1(R^+), \qquad X^0_{\mathcal{N}} = S_{\mathcal{N}} \cap H^1_0(R^+).$$

Then the Legendre spectral element/Laguerre spectral coupled approximation to problem (2.1) reads: Find $u_{\mathcal{N}} \in X^0_{\mathcal{N}}$ such that

$$a(u_{\mathcal{N}}, v_{\mathcal{N}}) = (f, v_{\mathcal{N}}) \quad \forall v_{\mathcal{N}} \in X^0_{\mathcal{N}}, \tag{2.2}$$

where $a(u_{\mathcal{N}}, v_{\mathcal{N}}) = (\partial_x u_{\mathcal{N}}, \partial_x v_{\mathcal{N}}) + \alpha(u_{\mathcal{N}}, v_{\mathcal{N}})$.

Before going into the details about the computational process of this approximation, we first investigate the convergence behavior of the numerical solution.

2.2. Error estimation

In order to carry out the error analysis for the approximation problem (2.2), we need some preliminary approximation results. We start with some notations and definitions. We denote $\omega_r(x) = (x-a)^r e^{a-x}$, $\hat{\omega}_r(x) = (x-a)^r$. In particular, we set $\omega(x) = \omega_0(x)$, $\hat{\omega}(x) = \hat{\omega}_0(x)$.

For any non-negative integer r, we define two spaces

$$\hat{A}^r(R_a^+) := \{v;\ v \text{ is measurable on } R_a^+ \text{ and } \|v\|_{\hat{A}^r(R_a^+)} < \infty\},$$
$$A^r(R_a^+) := \{v;\ v \text{ is measurable on } R_a^+ \text{ and } \|v\|_{A^r(R_a^+)} < \infty\},$$

equipped respectively with the following norms

$$\|v\|_{\hat{A}^r(R_a^+)} = \left(\sum_{k=0}^{r} |v|^2_{\hat{A}^k,R_a^+}\right)^{\frac{1}{2}}, \quad \text{with } |v|_{\hat{A}^k,R_a^+} = \|\partial_x^k v\|_{0;\omega_k,R_a^+},$$
$$\|v\|_{A^r(R_a^+)} = \left(\sum_{k=0}^{r} \|\partial_x^k v\|^2_{0;\hat{\omega}_r,R_a^+}\right)^{\frac{1}{2}}.$$

Moreover, for $r \geq 1$, we introduce the space (cf. [9]),

$$B^r(R_a^+) := \{v;\ v \text{ is measurable on } R_a^+ \text{ and } \|v\|_{B^r(R_a^+)} < \infty\},$$

with norm

$$\|v\|_{B^r(R_a^+)} = \left(\sum_{k=0}^{r} \|(x-a)^{(r-1)/2}(x-a+1)^{1/2}\partial_x^k v\|^2_{0;R_a^+}\right)^{1/2}.$$

Now we define some useful projection operators and present the basic approximation results.

Let $\pi_N^{(k)}$ be the $L^2(\Lambda^k)$-orthogonal projector from $L^2(\Lambda^k)$ into $\mathbb{P}_N(\Lambda^k)$, defined by: for all $v \in L^2(\Lambda^k)$,

$$(v - \pi_N^{(k)} v, \phi)_{\Lambda^k} = 0, \quad \forall \phi \in \mathbb{P}_N(\Lambda^k).$$

Let π_M^+ be the L^2_ω-orthogonal projector from $\hat{L}^2(R_a^+)$ into $\mathbb{P}_M(R_a^+)$, defined by:

$$\int_a^\infty (v - \pi_M^+ v)\phi_M \omega \mathrm{d}x = 0, \quad \forall v \in \hat{L}^2(R_a^+),\ \forall \phi_M \in \mathbb{P}_M(R_a^+).$$

Then we define the operator $\hat{\pi}_M^+$ from $L^2(R_a^+)$ into $\hat{\mathbb{P}}_M(R_a^+)$ by (cf. [4]):

$$\hat{\pi}_M^+ v(x) = e^{(a-x)/2}\pi_M^+(v(x)e^{(x-a)/2}), \quad \forall v \in L^2(R_a^+).$$

It can be easily verified that

$$\int_a^\infty (\hat{\pi}_M^+ v - v)\phi_M \mathrm{d}x = \int_a^\infty \left(\pi_M^+\left(v(x)e^{\frac{x-a}{2}}\right) - v(x)e^{\frac{x-a}{2}}\right) e^{\frac{a-x}{2}}\phi_M \mathrm{d}x = 0, \quad \forall \phi_M \in \hat{\mathbb{P}}_M(R_a^+).$$

Consequently, $\hat{\pi}_M^+$ is the orthogonal projector from $L^2(R_a^+)$ into $\hat{\mathbb{P}}_M(R_a^+)$. We know from [10] that for any integer $r \geq 0$, $v \in A^r(R_a^+)$,

$$\|v - \hat{\pi}_M^+ v\|_{0;R_a^+} \lesssim M^{-r/2}|e^{(x-a)/2}v|_{\hat{A}^r(R_a^+)} \lesssim M^{-r/2}\|v\|_{A^r(R_a^+)}. \tag{2.3}$$

We define below two projectors with respect to the global domain R^+:

- $L^2(R^+)$-orthogonal projector $\pi_{\mathcal{N}} : L^2(R^+) \to S_{\mathcal{N}}$, such that for all $v \in L^2(R^+)$,

$$(v - \pi_{\mathcal{N}} v, \phi_{\mathcal{N}})_{R^+} = 0, \quad \forall \phi_{\mathcal{N}} \in S_{\mathcal{N}};$$

- $H_0^1(R^+)$-orthogonal projector $\pi_{\mathcal{N}}^{1,0} : H_0^1(R^+) \to X_{\mathcal{N}}^0$, such that for all $v \in H_0^1(R^+)$,

$$(\partial_x(v - \pi_{\mathcal{N}}^{1,0} v), \partial_x \phi_{\mathcal{N}})_{R^+} = 0, \quad \forall \phi_{\mathcal{N}} \in X_{\mathcal{N}}^0.$$

Then, we have the following approximation results.

Lemma 2.1 (*Cf. [8]*). *Let $r \geq 0$. Then for all $v \in H^r(\Lambda^k)$,*

$$\|v - \pi_N^{(k)} v\|_{0;\Lambda^k} \lesssim h_k^{\min(N+1,r)} N^{-r}\|v\|_{r;\Lambda^k}.$$

Let us define space $H^{r,s}(R^+)$ as follows

$$H^{r,s}(R^+) := \{v;\, v_{|\Lambda} \in H^r(\Lambda),\ v_{|R_a^+} \in A^s(R_a^+)\}.$$

Then we have

Lemma 2.2. *Let $r, s \geq 0$. For all $v \in H^{r,s}(R^+)$, it holds that*

$$\|v - \pi_{\mathcal{N}} v\|_{0;R^+} \lesssim h^{\min(N+1,r)} N^{-r} \|v\|_{r;\Lambda} + M^{-\frac{s}{2}} \|v\|_{A^s(R_a^+)}.$$

Proof. Let

$$\phi_v = \begin{cases} \pi_N^{(k)} v, & x \in \Lambda^k,\ k = 1, 2, \ldots, K, \\ \hat{\pi}_M^+ v, & x \in R_a^+. \end{cases}$$

Then $\phi_v \in S_{\mathcal{N}}$, and from (2.3) and Lemma 2.1 it holds

$$\begin{aligned} \|v - \pi_{\mathcal{N}} v\|_{0;R^+}^2 &\leq \|v - \phi_v\|_{0;R^+}^2 \\ &= \sum_{k=1}^{K} \|v - \pi_N^{(k)} v\|_{0;\Lambda^k}^2 + \|v - \hat{\pi}_M^+ v\|_{0;R_a^+}^2 \\ &\lesssim h^{2\min(N+1,r)} N^{-2r} \sum_{k=1}^{K} \|v\|_{r;\Lambda^k}^2 + M^{-s} |\mathrm{e}^{\frac{x-a}{2}} v|_{\hat{A}^s(R_a^+)}^2 \\ &\lesssim h^{2\min(N+1,r)} N^{-2r} \|v\|_{r;\Lambda}^2 + M^{-s} \|v\|_{A^s(R_a^+)}^2. \end{aligned}$$

The proof is completed. □

Lemma 2.3. *Let $r \geq 1, s \geq 1$. Then for all $v \in \{v;\, v_{|\Lambda} \in H^r(\Lambda),\ v_{|R_a^+} \in B^s(R_a^+)\} \cap H_0^1(R^+)$, we have the following estimate,*

$$\|v - \pi_{\mathcal{N}}^{1,0} v\|_{1;R^+} \lesssim h^{\min(N,r-1)} N^{1-r} \|v\|_{r;\Lambda} + M^{\frac{1}{2}-\frac{s}{2}} \|v\|_{B^s(R_a^+)}.$$

Proof. For all $v \in H_0^1(R^+)$, by the definition of $\pi_{\mathcal{N}}^{1,0}$, we have

$$\|v - \pi_{\mathcal{N}}^{1,0} v\|_{1;R^+} \lesssim |v - \pi_{\mathcal{N}}^{1,0} v|_{1;R^+} \leq \inf_{\phi \in X_{\mathcal{N}}^0} |v - \phi|_{1;R^+}.$$

We define the function ϕ by

$$\phi(x) = \begin{cases} \phi_1^k(x), & x \in \Lambda^k,\ k = 1, 2, \ldots, K, \\ \phi_2(x), & x \in R_a^+, \end{cases}$$

where

$$\begin{aligned} \phi_1^k(x) &= \int_{a_{k-1}}^{x} \pi_{N-1}^{(k)}(\partial_y v(y))\mathrm{d}y + v(a_{k-1}), \\ \phi_2(x) &= \mathrm{e}^{\frac{a-x}{2}} \left(\int_a^x \pi_{M-1}^+ \partial_y \left(\mathrm{e}^{\frac{y-a}{2}} v(y) \right) \mathrm{d}y + v(a) \right). \end{aligned}$$

Then it can be checked that

$$\begin{aligned} &\phi_1^k(a_k) = \phi_1^{k+1}(a_k) = v(a_k), \quad k = 1, 2, \ldots, K-1, \\ &\phi_1^K(a) = \phi_2(a) = v(a). \end{aligned}$$

This means

$$\phi \in X_{\mathcal{N}}^0, \quad (\phi - v)_{|\Lambda^k} \in H_0^1(\Lambda^k), \quad k = 1, 2, \ldots, K-1; \qquad (\phi - v)_{|R_a^+} \in H_0^1(R_a^+).$$

On the other hand, we can express v by

$$v(x) = \mathrm{e}^{\frac{a-x}{2}} \left(\int_a^x \partial_y \left(\mathrm{e}^{\frac{y-a}{2}} v(y) \right) \mathrm{d}y + v(a) \right), \quad x \in R_a^+.$$

Let $\chi(x) = e^{a-x}$. Then, combining Lemma 2.2 of [5] and the approximation results of the projectors $\pi_N^{(k)}$ and π_M^+, we have

$$\begin{aligned}
\|v - \pi_{\mathcal{N}}^{1,0} v\|_{1;R^+}^2 &\lesssim \sum_{k=1}^{K} |v - \phi_1^k|_{1;\Lambda^k}^2 + |v - \phi_2|_{1;R_a^+}^2 \\
&\lesssim \sum_{k=1}^{K} |v - \phi_1^k|_{1;\Lambda^k}^2 + |\chi^{-\frac{1}{2}}(v - \phi_2)|_{1;\chi,R_a^+}^2 \\
&= \sum_{k=1}^{K} \|\partial_x v - \pi_{N-1}^{(k)} \partial_x v\|_{1;\Lambda^k}^2 + \|\partial_x(\chi^{-\frac{1}{2}} v) - \pi_{M-1}^{+} \partial_x(\chi^{-\frac{1}{2}} v)\|_{0;\chi,R_a^+}^2 \\
&\lesssim h^{2\min(N,r-1)} N^{2-2r} \sum_{k=1}^{K} \|\partial_x v\|_{r-1;\Lambda_a^k}^2 + M^{1-s} |\partial_x(\chi^{-\frac{1}{2}} v)|_{\hat{A}^{s-1}(R_a^+)}^2 \\
&\lesssim h^{2\min(N,r-1)} N^{2-2r} \|v\|_{r;\Lambda}^2 + M^{1-s} \|v\|_{B^s(R_a^+)}^2 .
\end{aligned}$$

This completes the proof. □

We are now in a position to derive the error estimation.

Theorem 2.1. *Let $\alpha > 0$, $r \geq 1$ and $s \geq 1$. u and $u_{\mathcal{N}}$ are the solutions of (2.1) and (2.2) respectively. Then the following estimate holds*

$$\|u - u_{\mathcal{N}}\|_{1;R^+} \lesssim h^{\min(N,r-1)} N^{1-r} \|u\|_{r;\Lambda} + M^{\frac{1}{2}-\frac{s}{2}} \|u\|_{B^s(R_a^+)} .$$

Proof. Let $e_{\mathcal{N}} = u_{\mathcal{N}} - \pi_{\mathcal{N}}^{1,0} u$. By subtracting (2.2) from (2.1),

$$(\partial_x e_{\mathcal{N}}, \partial_x v_{\mathcal{N}}) + \alpha(e_{\mathcal{N}}, v_{\mathcal{N}}) = (\partial_x(u - \pi_{\mathcal{N}}^{1,0} u), \partial_x v_{\mathcal{N}}) + \alpha(u - \pi_{\mathcal{N}}^{1,0} u, v_{\mathcal{N}}), \quad \forall v_{\mathcal{N}} \in X_{\mathcal{N}}^0 .$$

Taking $v_{\mathcal{N}} = e_{\mathcal{N}}$ in the above equation, we find

$$\min(1, \alpha) \|e_{\mathcal{N}}\|_{1;R^+}^2 \leq \alpha(u - \pi_{\mathcal{N}}^{1,0} u, e_{\mathcal{N}}) \leq \alpha \|u - \pi_{\mathcal{N}}^{1,0} u\|_{1;R^+} \|e_{\mathcal{N}}\|_{1;R^+} .$$

This gives

$$\|e_{\mathcal{N}}\|_{1;R^+} \lesssim \|u - \pi_{\mathcal{N}}^{1,0} u\|_{1;R^+} .$$

Finally, by using the triangle inequality and Lemma 2.3, we obtain

$$\begin{aligned}
\|u - u_{\mathcal{N}}\|_{1;R^+} &\leq \|u - \pi_{\mathcal{N}}^{1,0} u\|_{1;R^+} + \|e_{\mathcal{N}}\|_{1;R^+} \lesssim \|u - \pi_{\mathcal{N}}^{1,0} u\|_{1;R^+} \\
&\lesssim h^{\min(N,r-1)} N^{1-r} \|u\|_{r;\Lambda} + M^{\frac{1}{2}-\frac{s}{2}} \|u\|_{B^s(R_a^+)} . \quad \square
\end{aligned}$$

2.3. Implementation: a Schur complement method

Now we give the detailed computational process of the discrete problem (2.2). Let

$$\mathring{V}_N^k := \mathbb{P}_N(\Lambda^k) \cap H_0^1(\Lambda^k), \quad k = 1, 2, \ldots, K; \qquad \mathring{W}_M := \hat{\mathbb{P}}_M(R_a^+) \cap H_0^1(R_a^+).$$

To construct a suitable basis for the approximation space, we will use the orthogonality of the Legendre and Laguerre polynomials. First we transform the physical domain Λ^k to the reference domain $\hat{\Lambda} = (-1, 1)$ by the coordinate transformation as follows:

$$\hat{x}_k := \hat{x}_k(x) = \frac{2}{h_k} x - \frac{a_k + a_{k-1}}{h_k}, \quad \forall x \in \Lambda^k .$$

Then following [11,4], we define

$$\phi_j^k(x) = \begin{cases} \dfrac{1}{\sqrt{4j+6}} (L_j(\hat{x}_k) - L_{j+2}(\hat{x}_k)), & x \in \Lambda^k, \\ 0, & \text{others}, \end{cases} \quad j = 0, 1, \ldots, N-2, \; k = 1, 2, \ldots, K;$$

$$\hat{\phi}_j(x) = \begin{cases} \hat{\mathcal{L}}_j(x-a) - \hat{\mathcal{L}}_{j+1}(x-a), & x \in R_a^+, \\ 0, & \text{others}, \end{cases} \quad j = 0, 1, \ldots, M-1,$$

where $L_j(x)$ is the Legendre polynomial of degree j. It is readily seen that

$$\mathring{V}_N^k = \text{span}\{\phi_0^k(x), \phi_1^k(x), \ldots, \phi_{N-2}^k(x)\}, \quad k = 1, 2, \ldots, K;$$
$$\mathring{W}_M = \text{span}\{\hat{\phi}_0(x), \hat{\phi}_1(x), \ldots, \hat{\phi}_{M-1}(x)\}.$$

Defining the space

$$\mathring{X}_{\mathcal{N}} = \{v;\, v_{|\Lambda^k} \in \mathring{V}_N^k,\ k = 1, 2, \ldots, K;\, v_{|R_a^+} \in \mathring{W}_M\},$$

we now construct the basis functions $\varphi_1, \varphi_2, \ldots, \varphi_K$ corresponding respectively to the interfacial nodes $a_1, a_2, \ldots, a_K$, such that

$$X_{\mathcal{N}}^0 = \mathring{X}_{\mathcal{N}} \oplus \text{span}\{\varphi_1, \varphi_2, \ldots, \varphi_K\}.$$

To this end we define $\varphi_k,\ k = 1, 2, \ldots, K-1$, as follows:

$$\varphi_k(x) = \begin{cases} \frac{1}{2}(L_0(\hat{x}_k) + L_1(\hat{x}_k)), & x \in \Lambda^k, \\ \frac{1}{2}(L_0(\hat{x}_{k+1}) - L_1(\hat{x}_{k+1})), & x \in \Lambda^{k+1}, \\ 0, & \text{others}, \end{cases}$$

and set

$$\varphi_K(x) = \begin{cases} \frac{1}{2}(L_0(\hat{x}_K) + L_1(\hat{x}_K)), & x \in \Lambda^K, \\ \frac{3}{2}\hat{\mathcal{L}}_0(x-a) - \frac{1}{2}\hat{\mathcal{L}}_1(x-a), & x \in R_a^+, \\ 0, & \text{others}. \end{cases}$$

Then it is verified that

$$\varphi_k \in X_{\mathcal{N}}^0, \quad \varphi_k(a_k) = 1.$$

Moreover, all φ_k, together with $\phi_j^k,\ j = 0, 1, \ldots, N-2,\ k = 1, 2, \ldots, K$, and $\hat{\phi}_j,\ j = 0, 1, \ldots, M-1$ are linearly independent, and form a basis of $X_{\mathcal{N}}^0$.

Next we employ the idea, used in [12] in the frame of a dual-Petrov–Galerkin method for third-order equations, to solve our coupled spectral approximation problem (2.2). The computational process consists of the following steps:

- Complement space. In this step we construct the orthogonal complement of the space $\mathring{X}_{\mathcal{N}}$ with respect to the bilinear form $a(\cdot,\cdot)$. Let $\mathring{\varphi}_1, \mathring{\varphi}_2, \ldots, \mathring{\varphi}_K \in \mathring{X}_{\mathcal{N}}$ be the solutions of the following problems:

$$a(\mathring{\varphi}_k, \mathring{v}_{\mathcal{N}}) = -a(\varphi_k, \mathring{v}_{\mathcal{N}}), \quad \forall \mathring{v}_{\mathcal{N}} \in \mathring{X}_{\mathcal{N}},\ k = 1, 2, \ldots, K. \tag{2.4}$$

  Set $\Theta_k = \mathring{\varphi}_k + \varphi_k,\ k = 1, 2, \ldots, K$, and $\mathring{X}_{\mathcal{N}}^{\perp} = \text{span}\{\Theta_1, \Theta_2, \ldots, \Theta_K\}$. Then it is immediate that space $\mathring{X}_{\mathcal{N}}^{\perp}$ is orthogonal to space $\mathring{X}_{\mathcal{N}}$ in the sense that

$$a(\varphi_{\mathcal{N}}, v_{\mathcal{N}}) = 0, \quad \forall \varphi_{\mathcal{N}} \in \mathring{X}_{\mathcal{N}}^{\perp},\ v_{\mathcal{N}} \in \mathring{X}_{\mathcal{N}}.$$

- Solve the Schur complement problem for the values at the interfacial nodes $a_1, a_2, \ldots, a_K$:

$$\sum_{k=1}^{K} a(\Theta_k, \Theta_j) u_{\mathcal{N}}(a_k) = (f, \Theta_j), \quad j = 1, 2, \ldots, K. \tag{2.5}$$

- Solve the subproblems for the values at the interior nodes of each subdomain: Find $\mathring{u}_{\mathcal{N}} \in \mathring{X}_{\mathcal{N}}$, such that

$$a(\mathring{u}_{\mathcal{N}}, \mathring{v}_{\mathcal{N}}) = (f, \mathring{v}_{\mathcal{N}}), \quad \forall \mathring{v}_{\mathcal{N}} \in \mathring{X}_{\mathcal{N}}. \tag{2.6}$$

- Assemblage: Let $u_{\mathcal{N}} = \mathring{u}_{\mathcal{N}} + \sum_{k=1}^{K} u_{\mathcal{N}}(a_k)\Theta_k$. Then for all $v_{\mathcal{N}}$ there exist $\mathring{v}_{\mathcal{N}} \in \mathring{X}_{\mathcal{N}}$ and $v_{\mathcal{N}}^{\perp} \in \mathring{X}_{\mathcal{N}}^{\perp}$ such that $v_{\mathcal{N}} = \mathring{v}_{\mathcal{N}} + v_{\mathcal{N}}^{\perp}$, and consequently

$$\begin{aligned} a(u_{\mathcal{N}}, v_{\mathcal{N}}) &= a\left(\mathring{u}_{\mathcal{N}} + \sum_{k=1}^{K} u_{\mathcal{N}}(a_k)\Theta_k,\ \mathring{v}_{\mathcal{N}} + v_{\mathcal{N}}^{\perp}\right) \\ &= a(\mathring{u}_{\mathcal{N}}, \mathring{v}_{\mathcal{N}}) + a(\mathring{u}_{\mathcal{N}}, v_{\mathcal{N}}^{\perp}) + \sum_{k=1}^{K} u_{\mathcal{N}}(a_k) a(\Theta_k, \mathring{v}_{\mathcal{N}}) + \sum_{k=1}^{K} u_{\mathcal{N}}(a_k) a(\Theta_k, v_{\mathcal{N}}^{\perp}) \\ &= (f, \mathring{v}_{\mathcal{N}}) + (f, v_{\mathcal{N}}^{\perp}) \\ &= (f, v_{\mathcal{N}}). \end{aligned}$$

  In the above, we have used the fact that $a(\mathring{u}_{\mathcal{N}}, v_{\mathcal{N}}^{\perp}) = 0$ and $a(\Theta_k, \mathring{v}_{\mathcal{N}}) = 0$ due to the orthogonality. Thus $\mathring{u}_{\mathcal{N}} + \sum_{k=1}^{K} u_{\mathcal{N}}(a_k)\Theta_k$ is the solution we are seeking.

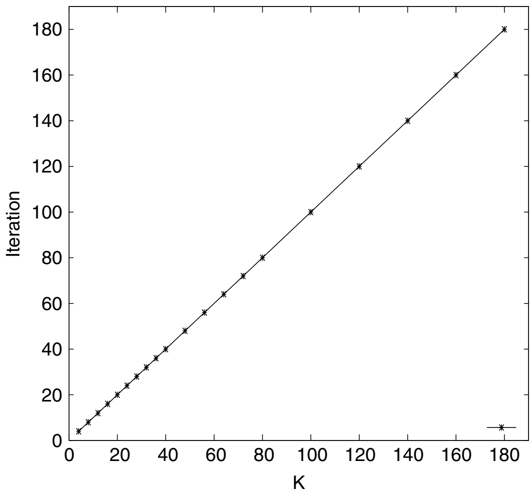

Fig. 1. Iteration numbers of the conjugate gradient for the Schur complement versus K.

From the above algorithm we see that problem (2.2) is decomposed into some smaller subproblems: two sets of elemental problems (2.4) and (2.6), and one Schur complement problem (2.5). Note that problem (2.6) can be completely split into K independent subproblems. Thus the computational process is very efficient. To derive the matrix statements of these problems, we denote

$$u_{\mathcal{N}}(x)_{|\Lambda^k} = \sum_{i=0}^{N-2} \hat{u}_i^k \phi_i^k(x), \qquad U^k = (\hat{u}_1^k, \hat{u}_2^k, \dots, \hat{u}_{N-2}^k)^T;$$
$$u_{\mathcal{N}}(x)_{|R_a^+} = \sum_{i=0}^{M-1} \hat{u}_i^+ \hat{\phi}_i(x), \qquad U^+ = (\hat{u}_1^+, \hat{u}_2^+, \dots, \hat{u}_{M-2}^+)^T;$$
$$B_{ji}^k = (\phi_i^k, \phi_j^k)_{\Lambda^k}, \qquad A_{ji}^k = (\phi_i^{k'}, \phi_j^{k'})_{\Lambda^k}, \qquad B_{ji}^+ = (\hat{\phi}_i, \hat{\phi}_j)_{R_a^+}, \qquad A_{ji}^+ = (\hat{\phi}_i', \hat{\phi}_j')_{R_a^+};$$
$$B^k = (B_{ji}^k)_{0\le i,\, j\le N-2}, \qquad A^k = (A_{ji}^k)_{0\le i,\, j\le N-2}, \qquad B^+ = (B_{ji}^+)_{0\le i,\, j\le M-1}, \qquad A^+ = (A_{ji}^+)_{0\le i,\, j\le M-1}.$$

By bringing the above expressions into (2.4) and (2.6), we obtain the following linear systems:

$$(\alpha B^k + A^k)U^k = F^k, \quad k = 1, 2, \dots, K,$$
$$(\alpha B^+ + A^+)U^+ = F^+,$$

where $F^k = (f_1^k, f_2^k, \dots, f_{N-2}^k)^T$, with $f_j^k = (f, \phi_i^k)_{\Lambda^k}$. Similarly for F^+. By the orthogonality of the Legendre polynomials and Laguerre functions respectively, it can be easily verified that the coefficient matrices of the above systems are respectively pentagonal and triangular. On the other side, the matrix for the interfacial unknowns is full, but has small dimension (generally K is small). A natural choice for solving the linear system on the interfacial unknowns is the conjugate gradient iteration since the coefficient matrix is symmetric positive definite. The convergence behavior of this iteration method will be investigated by means of some numerical tests.

2.4. Numerical validation

2.4.1. Convergence test

Example 1. We consider problem (2.1) with an exact analytical solution:

$$u(x) = \sin(kx)e^{-\gamma x}, \tag{2.7}$$

where k is a constant describing the frequency of the solution, γ measures the decay speed as x tends to infinity. We first investigate the convergence property of the conjugate gradient method for the Schur complement system (2.5) in terms of the discrete parameters K, N, M. In Fig. 1 we plot the iteration numbers needed for the iteration method to reach the convergence tolerance as a function of the element number K. We observe a clear linear increase with increasing K in this figure. Moreover, further tests have shown that the convergence of the iteration is basically independent of the polynomial degrees N or M. This implies that the condition number of the coefficient matrix of (2.5) behaves as $O(K^2)$.

The next test concerns the investigation of the convergence property of the coupled spectral method. We fix $k = 8$, $\gamma = 1$, $a = 8$, and let vary N and/or M.

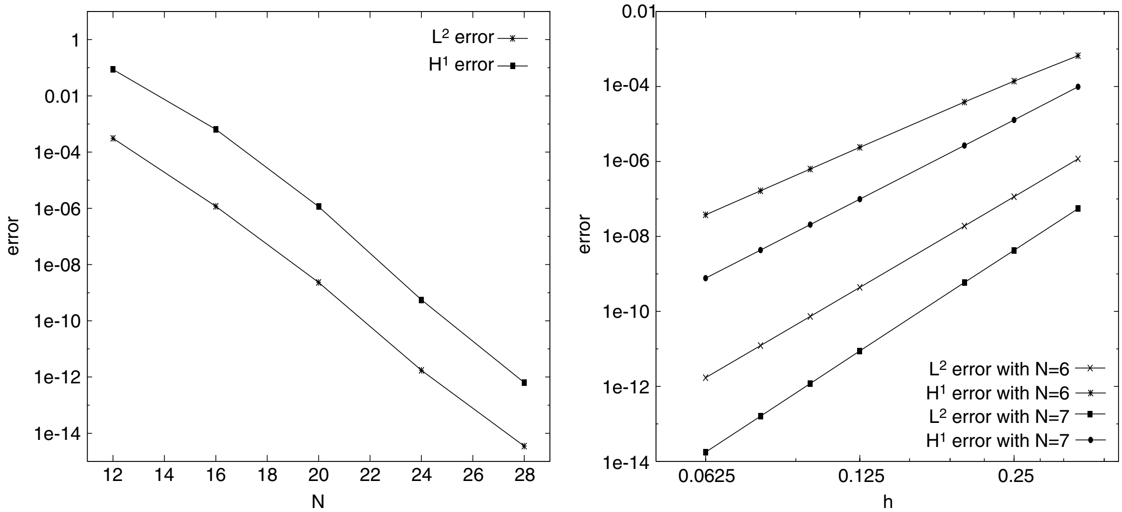

Fig. 2. Left: errors as a function of N; right: errors as a function of h.

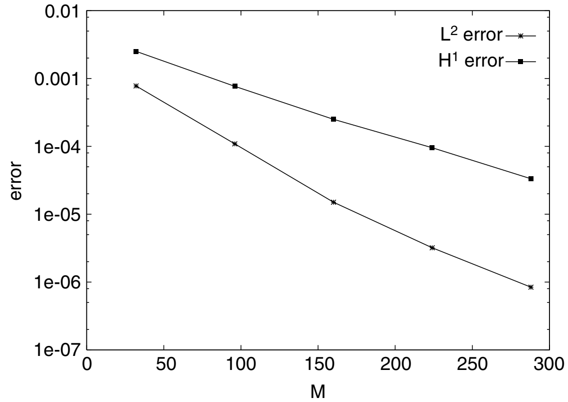

Fig. 3. Errors as a function of M.

- Fix $M = 320$. This M has been checked large enough such that the error from the Laguerre domain is negligible. In Fig. 2(left), we plot the errors in Λ as a function of the polynomial degree N with $K = 4$. A logarithmic scale is used for the error-axis. Clearly, the errors show an exponential decay, since one observes that the error variations are essentially linear versus the polynomial degree. That is the so-called spectral convergence as expected for a smooth exact solution. In Fig. 2(right), we plot in a log–log scale the errors in Λ as a function of h with $N = 6$ and $N = 7$ respectively. The obvious linear decrease in this log–log plot indicates that the convergence with respect to h is algebraic, as predicted by the theoretical estimates.
- We now fix $N = 32$ and $K = 4$ to avoid error contamination from the Legendre approximation in Λ. In Fig. 3 we present in semi-logarithmic scale, the errors in R_a^+ as a function of M. It is clear that the errors show an exponential decay, indicating the spectral accuracy of the Laguerre approximation in the infinite subdomain R_a^+.

Example 2. We test for an algebraic decay solution as follows:

$$u(x) = \frac{\sin(kx)}{(1+x)^{\gamma}}, \tag{2.8}$$

where k is temporarily fixed to 4, γ to 3.5. This solution is expected to be more difficult to capture since it shows slower decay at infinity than the previous solution. We repeat below the same tests as in Example 1.

- $M = 320$. We give in Fig. 4(left) the errors in Λ versus N with $K = 4$. Once again, the numerical solution converges exponentially to the exact solution in Λ as N increases.
  Fig. 4(right) shows the errors in the log–log scale as a function of h in Λ with $N = 6$ and $N = 7$ respectively. We see then an algebraic convergence, as we have explained in Example 1.

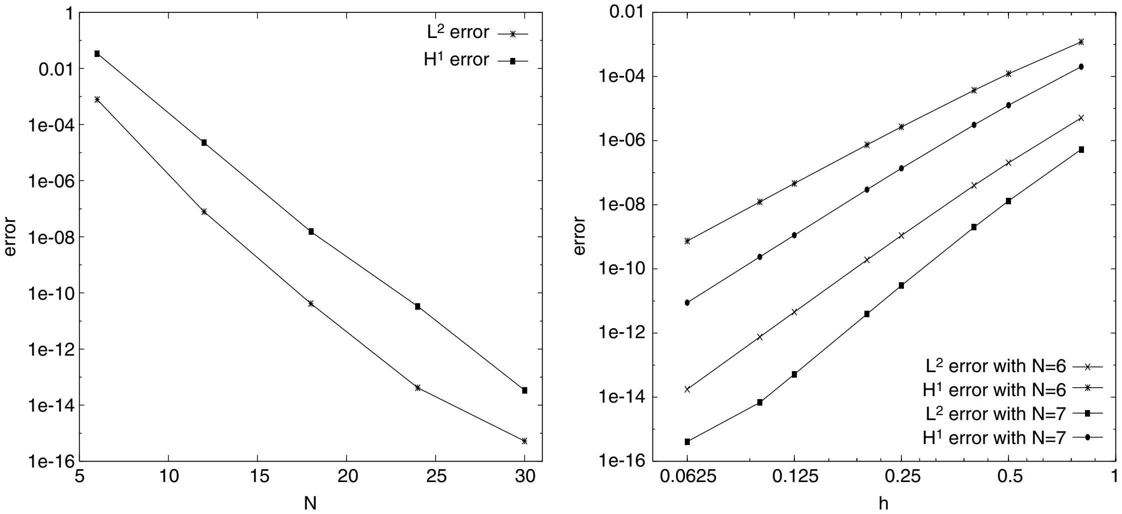

Fig. 4. Left: errors as a function of N; right: errors as a function of h.

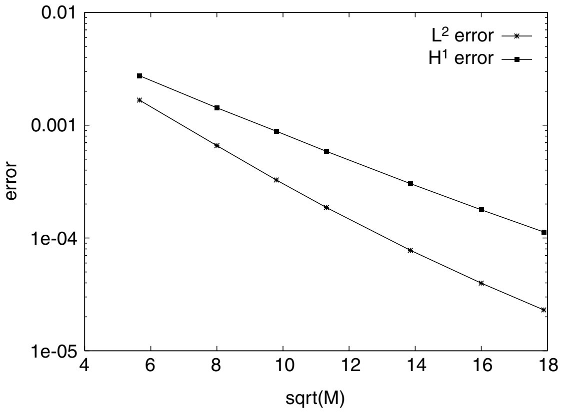

Fig. 5. Errors in R_a^+ as a function of M.

- $N = 32$, $K = 4$. We plot in Fig. 5 the errors in R_a^+ as a function of M. Although there is a slow decay feature of the solution in R_a^+, we still observe an exponential convergence with respect to the degree of the Laguerre function.

2.4.2. Comparison with pure Laguerre method

We now make a comparison on the accuracy of our coupled method to the pure Laguerre–Galerkin method proposed in [4] as follows: Find $u_M \in \hat{X}_M = H_0^1(R^+) \cap \mathbb{P}_M(R^+)$, such that

$$(\partial_x u_M, \partial_x v_M) + \alpha(u_M, v_M) = (f, v_M) \quad \forall v_M \in \hat{X}_M. \tag{2.9}$$

In this pure Laguerre method, the Laguerre polynomials are used to approximate the solution in the whole infinite domain.

We first employ the method (2.9) to approximate the solutions given in Examples 1 and 2.

- In Fig. 6(left), we plot the errors as a function of M for the exact solution (2.7) with $k = 3, 4$, $\gamma = 1, 2$ respectively. It is clear that the convergence rate remains exponential for all these smooth solutions.
- In Fig. 6(right), we show the results using (2.8) with $k = 3, 4$, $\gamma = 3.5, 4.5$. In this case we obtain only algebraic convergences, which is in full consistency with the limited regularity of the exact solutions.

From Fig. 6, we observe that in the pure Laguerre approximation the convergence quickly slows down as the exact solution has higher frequency, i.e., bigger k, or shows slower decay as x tends to infinity, i.e., smaller γ. An explanation of this phenomena is, as shown in Fig. 7, that the distance between adjacent Laguerre–Gauss points increases very fast as M increases.

We now compare the numerical results obtained respectively by our coupled method and the pure Laguerre method for the solutions in Example 1 with $\gamma = 2$, $k = 5, 10$. The parameters used are $a = 16$, $K = 8$, $N = 16$, and $M = 192$ for the

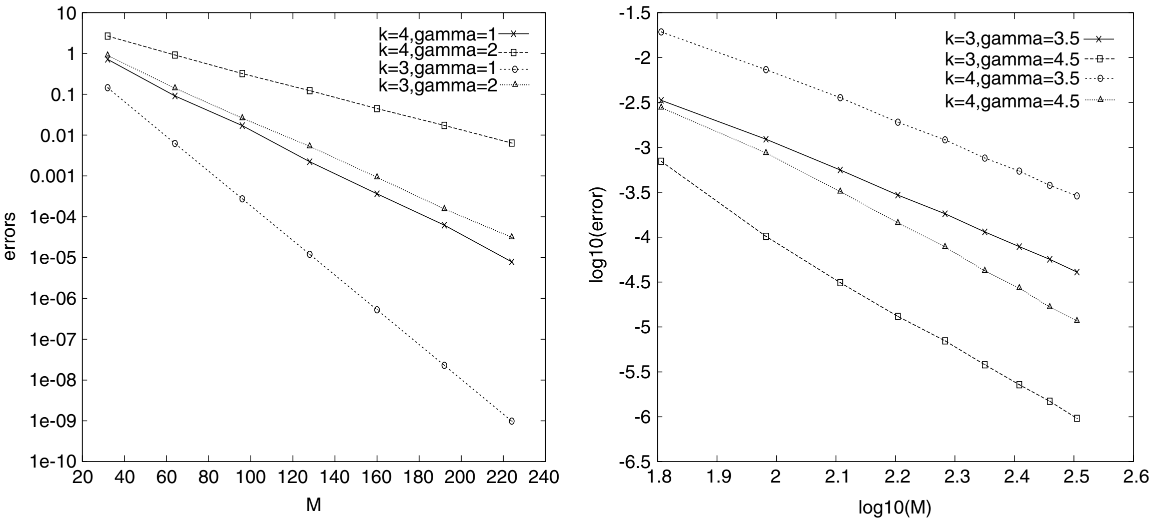

Fig. 6. H^1-norm as a function of M: left, Example 1; right, Example 2.

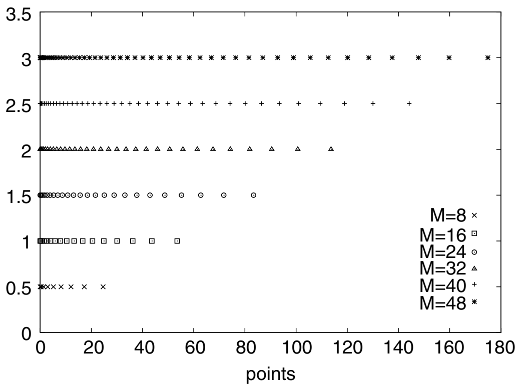

Fig. 7. Distribution of Laguerre–Gauss points.

coupled method, and $M = 320$ for the pure Laguerre method. Note that in order to make the comparisons reasonable, the discretization parameters have been chosen such that the total grid points for both methods are nearly the same. The errors of the numerical solutions by the two methods are compared in Fig. 8, from which we see that the coupled method provides a much more accurate numerical solution than the pure Laguerre method, especially for the high frequency solution in the upstream domain.

2.5. Remarks for equations with variable coefficients

We now consider the elliptic equation with variable coefficients as follows:

$$\partial_x(\beta(x)\partial_x u) + \alpha(x)u = f$$

where $\alpha(x)$ and $\beta(x)$ are two positive coefficients depending on x. In this case, the fast evaluation of the integrals involving in the weak formulation is no longer available because the basis functions constructed in Section 2.3 are not orthogonal with respect to the coefficients $\alpha(x)$ and $\beta(x)$. Nevertheless, the Schur complement technique presented in Section 2.3 remains applicable. The only difference is that in this case the integrals should be computed by using a Gauss–Lobatto/Gauss quadrature and it is recommended to use suitable nodal basis functions instead of the modal basis.

3. Coupled spectral methods for fourth-order equations

In this section, we will consider coupled spectral approximations to a fourth-order equation. As is known, in the multi-domain computation of fourth-order equations, it is not easy to handle the continuity at the elemental interfaces. Previous work for such problems includes approaches based on overlapping domain decomposition or splitting the original

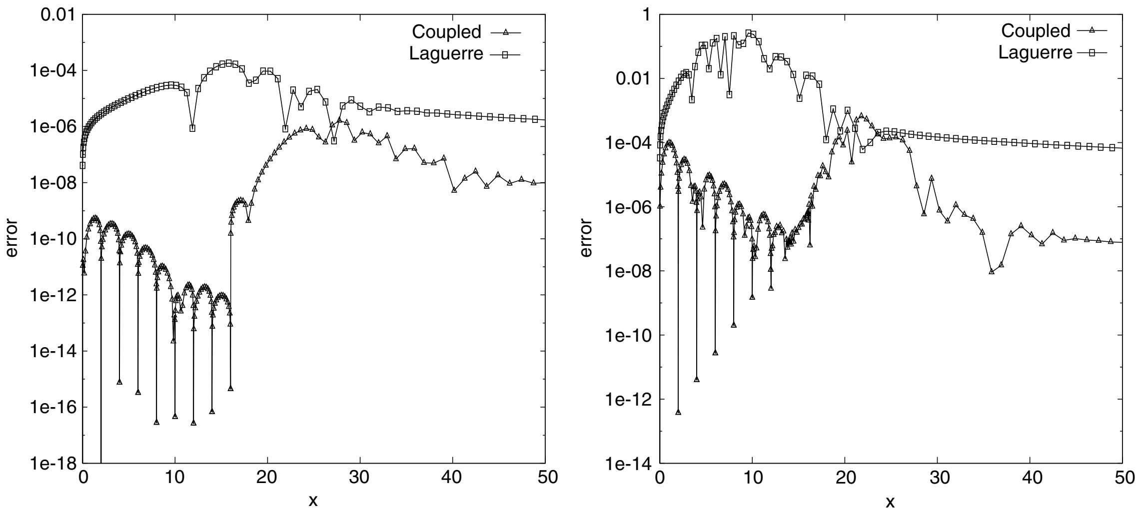

Fig. 8. Pointwise errors given by the coupled method and pure Laguerre method. Left: $k = 5$; right: $k = 10$.

equations into two second-order equations. We propose here a method based on non-overlapping domain decomposition. The implementation of the method employs the idea proposed in the previous sections for the second-order problem. The key to the efficiency of our algorithm is to construct appropriate basis functions, which lead to systems with sparse matrices for the discrete variational formulation. Error estimation of the approximation is also carried out. The efficiency and high accuracy of the proposed method is confirmed by some numerical tests, together with a comparison with a pure Laguerre approximation.

3.1. Problems and error estimation

We consider the following problem

$$\begin{cases} \partial_x^4 u - \alpha_1 \partial_x^2 u + \alpha_2 u = f, \quad x \in R^+, \\ u(0) = \partial_x u(0) = 0, \qquad \lim_{x\to+\infty} u(x) = \lim_{x\to+\infty} \partial_x u(x) = 0, \end{cases} \tag{3.1}$$

where $\alpha_1 > 0, \alpha_2 > 0$.

We define the approximation spaces

$$Y_{\mathcal{N}} = S_{\mathcal{N}} \cap H^2(R^+), \qquad Y^0_{\mathcal{N}} = S_{\mathcal{N}} \cap H^2_0(R^+),$$

where space $S_{\mathcal{N}}$ is defined in Section 2.

Then the Legendre spectral element/Laguerre spectral coupled method to problem (3.1) reads: Find $u_{\mathcal{N}} \in Y^0_{\mathcal{N}}$ such that

$$b(u_{\mathcal{N}}, v_{\mathcal{N}}) = (f, v_{\mathcal{N}}) \quad \forall v_{\mathcal{N}} \in Y^0_{\mathcal{N}}, \tag{3.2}$$

where

$$b(u, v) = (\partial_x^2 u, \partial_x^2 v) + \alpha_1(\partial_x u, \partial_x v) + \alpha_2(u, v).$$

In order to carry out the error analysis, we first define the orthogonal projection operator $\pi^2_{\mathcal{N}} : H^2(R^+) \to Y_{\mathcal{N}}$: for all $v \in H^2(R^+), \pi^2_{\mathcal{N}} v \in Y_{\mathcal{N}}$ is given by

$$(\partial_x^2(v - \pi^2_{\mathcal{N}} v), \partial_x^2 \phi) + (\partial_x(v - \pi^2_{\mathcal{N}} v), \partial_x \phi) + (v - \pi^2_{\mathcal{N}} v, \phi) = 0, \quad \forall \phi \in Y_{\mathcal{N}}. \tag{3.3}$$

We also define $\pi^{2,0}_{\mathcal{N}} : H^2_0(R^+) \to Y^0_{\mathcal{N}}$ by

$$(\partial_x^2(v - \pi^{2,0}_{\mathcal{N}} v), \partial_x^2 \phi) = 0, \quad \forall \phi \in Y^0_{\mathcal{N}}. \tag{3.4}$$

Lemma 3.1. *Let $r, s \geq 2$. Then for all $v \in \{v;\ v_{|\Lambda} \in H^r(\Lambda),\ \partial_x^2(\mathrm{e}^{\frac{x-a}{2}} v)_{|R^+_a} \in \hat{A}^{s-2}(R^+_a)\} \cap H^2(R^+)$,*

$$\|v - \pi^2_{\mathcal{N}} v\|_{2;R^+} \lesssim h^{\min(N-1,r-2)} N^{2-r} \|v\|_{r;\Lambda} + M^{1-\frac{s}{2}} |\partial_x^2(\mathrm{e}^{\frac{x-a}{2}} v)|_{\hat{A}^{s-2}(R^+_a)};$$

and for all $v \in \{v;\ v_{|\Lambda} \in H^r(\Lambda),\ \partial_x^2(\mathrm{e}^{\frac{x-a}{2}}v)_{|R_a^+} \in \hat{A}^{s-2}(R_a^+)\} \cap H_0^2(R^+)$,

$$\|v - \pi_{\mathcal{N}}^{2,0}v\|_{2;R^+} \lesssim h^{\min(N-1,r-2)}N^{2-r}\|v\|_{r;\Lambda} + M^{1-\frac{s}{2}}|\partial_x^2(\mathrm{e}^{\frac{x-a}{2}}v)|_{\hat{A}^{s-2}(R_a^+)}.$$

Proof. By the definition of $\pi_{\mathcal{N}}^2$, we have

$$\|v - \pi_{\mathcal{N}}^2 v\|_{2;R^+} \le \inf_{\phi \in Y_{\mathcal{N}}} \|v - \phi\|_{2;R^+}.$$

For all $v \in \{v;\ v_{|\Lambda} \in H^r(\Lambda),\ \partial_x^2(\mathrm{e}^{\frac{x-a}{2}}v)_{|R_a^+} \in \hat{A}^{s-2}(R_a^+)\} \cap H^2(R^+)$, let

$$\phi(x) = \begin{cases} \phi_1^k(x), & x \in \Lambda^k,\ k = 1, 2, \ldots, K, \\ \phi_2(x), & x \in R_a^+, \end{cases}$$

where

$$\phi_1^k(x) = \int_{a_{k-1}}^x \int_{a_{k-1}}^z \pi_{N-2}^{(k)}\partial_y^2 v\,\mathrm{d}y\mathrm{d}z + v(a_{k-1}) + \partial_x v(a_{k-1})(x - a_{k-1}),$$

$$\phi_2(x) = \mathrm{e}^{\frac{a-x}{2}}\left[\int_a^x \left(\int_a^z \pi_{M-2}^+\partial_y^2\left(\mathrm{e}^{\frac{y-a}{2}}v\right)\mathrm{d}y\right)\mathrm{d}z + \left(\partial_x v + \frac{v}{2}\right)(a)(x-a) + v(a)\right].$$

Then it can be verified that

$$\phi_1^k(a_k) = \phi_1^{k+1}(a_k) = v(a_k), \qquad (\phi_1^k)'(a_k) = (\phi_1^{k+1})'(a_k) = v'(a_k), \quad k = 1, 2, \ldots, K-1;$$
$$\phi_1^K(a) = \phi_2(a) = v(a), \qquad (\phi_1^K)'(a) = \phi_2'(a) = v'(a).$$

On the other hand, we have

$$v(x) = \mathrm{e}^{\frac{a-x}{2}}\left[\int_a^x \left(\int_a^z \partial_y^2\left(\mathrm{e}^{\frac{y-a}{2}}v\right)\mathrm{d}y\right)\mathrm{d}z + \left(\partial_x v + \frac{v}{2}\right)(a)(x-a) + v(a)\right], \quad x \in R_a^+.$$

A direct consequence of the above equalities is:

$$\phi \in Y_{\mathcal{N}}^0, \qquad (\phi - v)_{|\Lambda^k} \in H_0^2(\Lambda^k), \quad k = 1, 2, \ldots, K, \qquad (\phi - v)_{|R_a^+} \in H_0^2(R_a^+).$$

Moreover, by Lemma 2.2 of [5] and the approximation results of the projectors $\pi_N^{(k)}$ and π_M^+, we have

$$\begin{aligned}
\|v - \pi_{\mathcal{N}}^2 v\|_{2;R^+}^2 &\le \sum_{k=1}^K \|v - \phi_1^k\|_{2;\Lambda^k}^2 + \|v - \phi_2\|_{2;R_a^+}^2 \\
&\lesssim \sum_{k=1}^K |v - \phi_1^k|_{2;\Lambda^k}^2 + |\chi^{-\frac{1}{2}}(v - \phi_2)|_{2;\chi,R_a^+}^2 \\
&= \sum_{k=1}^K \|\partial_x^2 v - \pi_{N-2}^{(k)}\partial_x^2 v\|_{2;\Lambda^k}^2 + \|\partial_x^2(\chi^{-\frac{1}{2}}v) - \pi_{M-2}^+\partial_x^2(\chi^{-\frac{1}{2}}v)\|_{0;\chi,R_a^+}^2 \\
&\lesssim h^{2\min(N-1,r-2)}N^{4-2r}\sum_{k=1}^K \|\partial_x^2 v\|_{r-2;\Lambda^k}^2 + M^{2-s}|\partial_x^2(\chi^{-\frac{1}{2}}v)|_{\hat{A}^{s-2}(R_a^+)}^2 \\
&\lesssim h^{2\min(N-1,r-2)}N^{4-2r}\|v\|_{r;\Lambda}^2 + M^{2-s}|\partial_x^2(\mathrm{e}^{\frac{x-a}{2}}v)|_{\hat{A}^{s-2}(R_a^+)}^2.
\end{aligned}$$

Thus the first estimate is obtained. The second estimate can be proved similarly. □

By Lemma 3.1 and the following standard result for the approximation (3.1):

$$\|u - u_{\mathcal{N}}\|_{2;R^+} \lesssim \|v - \pi_{\mathcal{N}}^{2,0}v\|_{2;R^+},$$

we derive immediately the error estimate as follows.

Theorem 3.1. *Let u and $u_{\mathcal{N}}$ be respectively the solution of (3.1) and (3.2). Then*

$$\|u - u_{\mathcal{N}}\|_{2;R^+} \lesssim h^{\min(N-1,r-2)}N^{2-r}\|v\|_{r;\Lambda} + M^{1-\frac{s}{2}}|\partial_x^2(\mathrm{e}^{\frac{x-a}{2}}v)|_{\hat{A}^{s-2}(R_a^+)}.$$

3.2. Implementation

Let

$$\mathring{V}_N^k := \mathbb{P}_N(\Lambda^k) \cap H_0^2(\Lambda^k), \quad k = 1, 2, \ldots, K; \qquad \mathring{W}_M := \hat{\mathbb{P}}_M(R_a^+) \cap H_0^2(R_a^+).$$

We construct the basis functions: for $0 \le i \le N-4, 0 \le j \le M-2$,

$$\phi_i^k(x) = \begin{cases} \frac{1}{\sqrt{2(2i+3)^2(2i+5)}} \left(L_i(\hat{x}_k) - \frac{2(2i+5)}{2i+7} L_{i+2}(\hat{x}_k) + \frac{2i+3}{2i+7} L_{i+4}(\hat{x}_k) \right), & x \in \Lambda^k, \\ 0, & \text{others}, \end{cases}$$

$$\hat{\phi}_j(x) = \begin{cases} \hat{\mathcal{L}}_j(x-a) - 2\hat{\mathcal{L}}_{j+1}(x-a) + \hat{\mathcal{L}}_{j+2}(x-a), & x \in R_a^+, \\ 0, & \text{others}. \end{cases}$$

Following [11,4], it can be proved that

$$\mathring{V}_N^k = \text{span}\{\phi_0^k(x), \phi_1^k(x), \dots, \phi_{N-4}^k(x)\}, \quad k = 1, 2, \dots, K;$$
$$\mathring{W}_M = \text{span}\{\hat{\phi}_0(x), \hat{\phi}_1(x), \dots, \hat{\phi}_{M-2}(x)\}.$$

Let us now denote

$$\mathring{Y}_{\mathcal{N}} = \{v;\, v_{|\Lambda^k} \in \mathring{V}_N^k,\ k = 1, 2, \dots, K;\, v_{|R_a^+} \in \mathring{W}_M\}.$$

Then we construct the basis functions $\varphi_k, \psi_k,\ k = 1, 2, \dots, K$, associated to the interfacial nodes $a_1, a_2, \dots, a_K$, such that

$$Y_{\mathcal{N}}^0 = \mathring{Y}_{\mathcal{N}} \oplus \text{span}\{\varphi_1, \varphi_2, \dots, \varphi_K, \psi_1, \psi_2, \dots, \psi_K\}.$$

This can be done by asking $\varphi_k, \psi_k,\ k = 1, 2, \dots, K$ to satisfy:

$$\begin{cases} \varphi_k \in Y_{\mathcal{N}}^0, & \varphi_k(a_k) = 1, & \varphi_k'(a_k) = 0, \\ \psi_k \in Y_{\mathcal{N}}^0, & \psi_k(a_k) = 0, & \psi_k'(a_k) = 1, \end{cases} \quad k = 1, 2, \dots, K.$$

It can be checked that the following functions meet the requirement:

$$\varphi_k = \begin{cases} \frac{1}{2} L_0(\hat{x}_k) + \frac{3}{5} L_1(\hat{x}_k) - \frac{1}{10} L_3(\hat{x}_k), & x \in \Lambda^k, \\ \frac{1}{2} L_0(\hat{x}_{k+1}) - \frac{3}{5} L_1(\hat{x}_{k+1}) + \frac{1}{10} L_3(\hat{x}_{k+1}), & x \in \Lambda^{k+1}, \\ 0, & \text{others}, \end{cases} \quad k = 1, 2, \dots, K-1;$$

$$\varphi_K = \begin{cases} \frac{1}{2} L_0(\hat{x}_K) + \frac{3}{5} L_1(\hat{x}_K) - \frac{1}{10} L_3(\hat{x}_K), & x \in \Lambda^K, \\ \frac{3}{2} \hat{\mathcal{L}}_0(x-a) - \frac{1}{2} \hat{\mathcal{L}}_1(x-a), & x \in R_a^+, \\ 0, & \text{others}. \end{cases}$$

$$\psi_k = \begin{cases} \frac{h_k}{2} \left(\frac{L_2(\hat{x}_k) - L_0(\hat{x}_k)}{6} + \frac{L_3(\hat{x}_k) - L_1(\hat{x}_k)}{10} \right), & x \in \Lambda^k, \\ \frac{h_{k+1}}{2} \left(\frac{L_0(\hat{x}_{k+1}) - L_2(\hat{x}_{k+1})}{6} + \frac{L_3(\hat{x}_{k+1}) - L_1(\hat{x}_{k+1})}{10} \right), & x \in \Lambda^{k+1}, \\ 0, & \text{others}, \end{cases} \quad k = 1, 2, \dots, K-1;$$

$$\psi_K = \begin{cases} \frac{h_K}{2} \left(\frac{L_2(\hat{x}_K) - L_0(\hat{x}_K)}{6} + \frac{L_3(\hat{x}_K) - L_1(\hat{x}_K)}{10} \right), & x \in \Lambda^K, \\ \hat{\mathcal{L}}_0(x-a) - \hat{\mathcal{L}}_1(x-a), & x \in R_a^+, \\ 0, & \text{others}. \end{cases}$$

Similar to the second-order equation, we solve problem (3.2) by the following process:

- Schur complement space: Construct the orthogonal complement of $\mathring{Y}_{\mathcal{N}}$ with respect to the bilinear form $b(\cdot, \cdot)$. Let $\mathring{\varphi}_k, \mathring{\psi}_k \in \mathring{Y}_{\mathcal{N}}$ be the solutions of the following problems:

$$\begin{cases} b(\mathring{\varphi}_k, \mathring{v}_{\mathcal{N}}) = -b(\varphi_k, \mathring{v}_{\mathcal{N}}), \\ b(\mathring{\psi}_k, \mathring{v}_{\mathcal{N}}) = -b(\psi_k, \mathring{v}_{\mathcal{N}}), \end{cases} \quad \forall \mathring{v}_{\mathcal{N}} \in \mathring{Y}_{\mathcal{N}},\ k = 1, 2, \dots, K. \tag{3.5}$$

  Set $\Theta_k = \mathring{\varphi}_k + \varphi_k$, $\Upsilon_k = \mathring{\psi}_k + \psi_k$, and $\mathring{Y}_{\mathcal{N}}^{\perp} = \text{span}\{\Theta_k, \Upsilon_k,\ k = 1, 2, \dots, K\}$. Then it is readily seen that space $\mathring{Y}_{\mathcal{N}}^{\perp}$ is orthogonal to space $\mathring{Y}_{\mathcal{N}}$ in the sense that

$$b(\varphi_{\mathcal{N}}, v_{\mathcal{N}}) = 0, \quad \forall \varphi_{\mathcal{N}} \in \mathring{Y}_{\mathcal{N}}^{\perp}\ v_{\mathcal{N}} \in \mathring{Y}_{\mathcal{N}}.$$

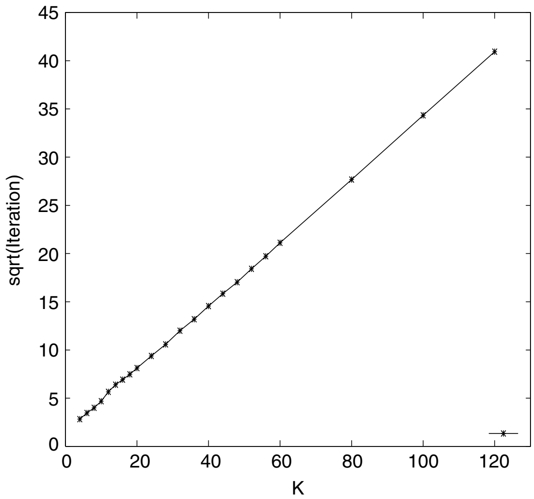

Fig. 9. Square of the iteration number of the conjugate gradient versus K.

- Solve the Schur complement problem for the unknowns $u_{\mathcal{N}}(a_k), u'_{\mathcal{N}}(a_i),\ k = 1, 2, \ldots, K$, associated to the interfacial nodes:

$$\begin{cases} \sum_{k=1}^{K} b(\Theta_k, \Theta_j) u_{\mathcal{N}}(a_k) + \sum_{k=1}^{K} b(\Upsilon_k, \Theta_j) u'_{\mathcal{N}}(a_k) = (f, \Theta_j), \quad j = 1, 2, \ldots, K, \\ \sum_{k=1}^{K} b(\Theta_k, \Upsilon_j) u_{\mathcal{N}}(a_k) + \sum_{k=1}^{K} b(\Upsilon_k, \Upsilon_j) u'_{\mathcal{N}}(a_k) = (f, \Upsilon_j), \quad j = 1, 2, \ldots, K. \end{cases} \tag{3.6}$$

- Solve subproblems for the values at the interior nodes of each subdomain: Find $\mathring{u}_{\mathcal{N}} \in \mathring{Y}_{\mathcal{N}}$ such that

$$b(\mathring{u}_{\mathcal{N}}, \mathring{v}_{\mathcal{N}}) = (f, \mathring{v}_{\mathcal{N}}), \quad \forall \mathring{v}_{\mathcal{N}} \in \mathring{Y}_{\mathcal{N}}. \tag{3.7}$$

- Assemblage: Let $u_{\mathcal{N}} = \mathring{u}_{\mathcal{N}} + \sum_{k=1}^{K} u_{\mathcal{N}}(a_k)\Theta_k + \sum_{k=1}^{K} u'_{\mathcal{N}}(a_k)\Upsilon_k$. Then by combining (3.5)–(3.7), we have

$$b(u_{\mathcal{N}}, v_{\mathcal{N}}) = (f, v_{\mathcal{N}}), \quad v_{\mathcal{N}} \in Y^0_{\mathcal{N}}.$$

  Thus the assembled $u_{\mathcal{N}}$ is the solution of (3.2).

As for the second-order problem, the fourth-order problem (3.2) is now split into some smaller systems: elemental subproblems (3.5) and (3.7), and the Schur complement problem (3.6) associated to the interfacial unknowns. Thanks to the orthogonality of the basis functions, subproblems (3.5) and (3.7) for all elements are sparse (enneahedral or pentagonal). Note that the Schur complement problem (3.6) has the same dimension as the element number, and can be solved by using the conjugate gradient iteration since the coefficient matrix is symmetric positive definite.

3.3. *Numerical validation*

3.3.1. *Convergence test*

We first consider the solution:

$$u(x) = \sin^2(kx)e^{-x}, \tag{3.8}$$

with $k = 2$ and $a = 16$ for the domain decomposition.

In Fig. 9 we plot the square of the iteration number of the conjugate gradient method for the Schur complement problem to reach the convergence. We find that the minimum iteration number behaves like $O(K^2)$. This dependence is stronger than what we have found for the second-order problem (only $O(K)$) for reasons unknown to us. Note that as for the second-order problem, the conjugate gradient iteration is insensitive to N or M.

Next we numerically investigate the discretization errors of the coupled spectral method.

- Fix $M = 320$, let N and h vary. We present in a semi-log scale in Fig. 10(left) the errors in H^2-norm in Λ as a function of N with $h = 0.5$ and $h = 0.8$. An exponential decay of the errors is observed, which is consistent with the theoretical estimate. In Fig. 10(right), we plot in a log–log scale the errors in Λ as a function of h with $N = 7$ and $N = 8$. It is observed that the error curves are straight lines in this full log representation. This indicates that the numerical solutions converge algebraically in h.

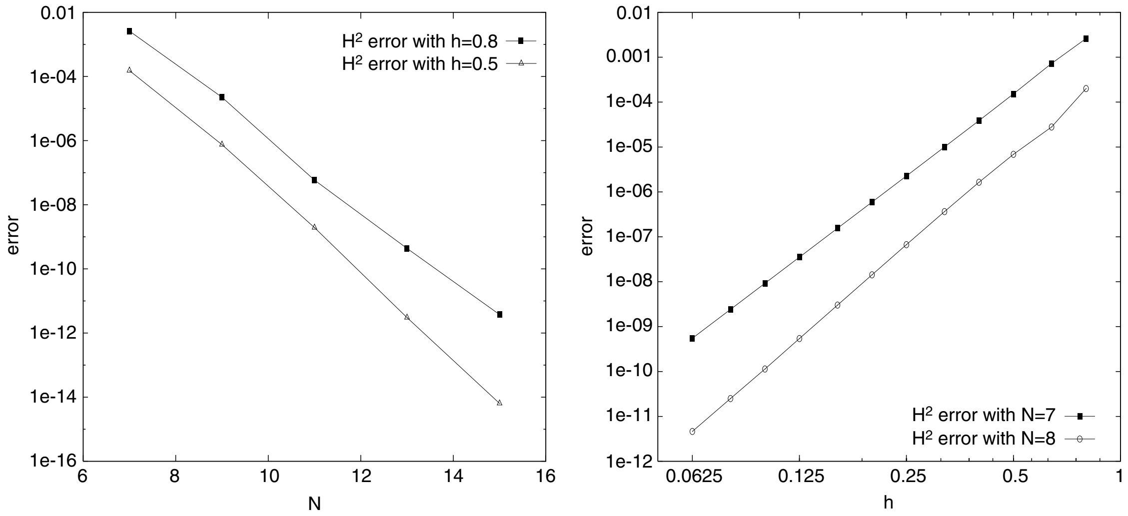

Fig. 10. Left: errors as a function of N; right: errors as a function of h.

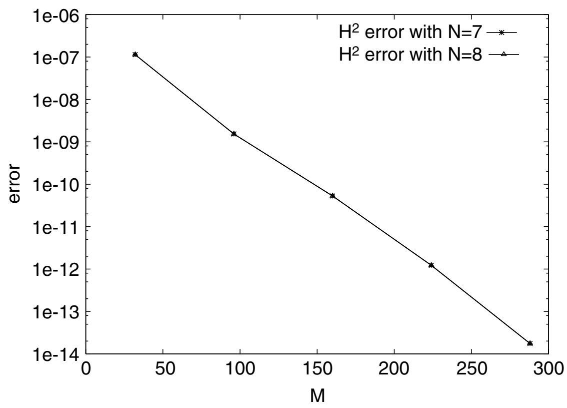

Fig. 11. Errors as a function of M.

- Fix h and N, let us vary M. Fig. 11 shows the errors in R_a^+ versus M in a semi-logarithmic scale. It is clear that the errors show an exponential decay. Furthermore, the fact that two different N give the same line means that the effect of N in this test is negligible.

3.3.2. Comparison with a pure Laguerre method

The coupled method is compared to a pure Laguerre method proposed in [4], which consists in seeking the numerical solution in the global polynomial space $\hat{Y}_M := \hat{\mathbb{P}}_M \cap H_0^2(R^+)$.

We first investigate the convergence behavior of this pure Laguerre approximation. In Fig. 12, we plot the errors versus M for the solution (3.8) with $k = 1$ and $k = 2$. It is seen that the convergence quickly slows down as k becomes bigger.

The efficiency of the coupled method can be demonstrated by comparing the accuracy for high frequency solutions. To this end, we take $k = 5, 10$ in (3.8), and compare the numerical solutions by both methods. The discretization parameters are chosen such that the total grid points are the same in both approximations. As shown in Fig. 13, the coupled approximation leads to much better results than the pure Laguerre method.

4. Concluding remarks

We have presented a complete analysis for the Legendre–Laguerre coupled spectral element method to the second- and fourth-order equations on the half line. Some error estimates are derived to demonstrate the spectral accuracy of the proposed methods. Moreover, we presented a fast algorithm for both problems, together with some numerical results to confirm the efficiency of the methods. A comparison with the pure Laguerre method indicates that the coupled approximation is more accurate, especially for high frequency problems. A particular advantage of the approach is that the decomposition point a can be chosen suitably according to the practical need.

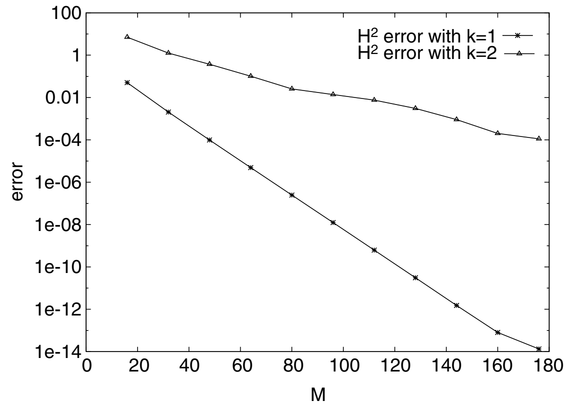

Fig. 12. Errors versus M by the pure Laguerre method.

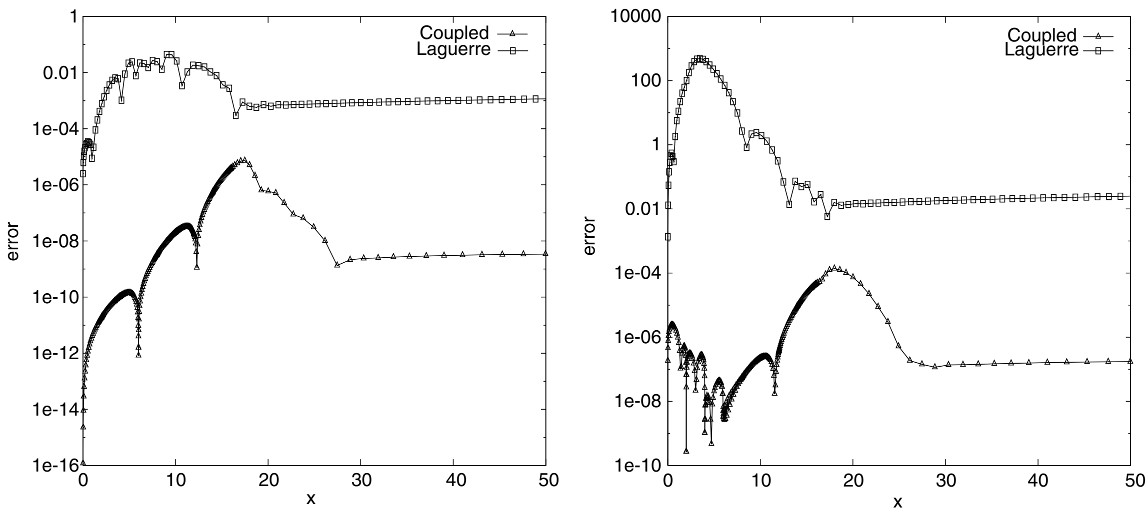

Fig. 13. Pointwise errors of the two methods. Left: $k = 5$; right: $k = 10$.

Acknowledgements

The work of first author is partially supported by the fund of Huaqiao University under grant 09BS105. The research of second author was partially supported by National NSF of China under Grant 10531080, and 973 High Performance Scientific Computation Research Program 2005CB321703.

References

[1] C. Mavriplis, Laguerre polynomials for infinite-domain spectral elements, Comput. Methods Appl. Mech. Engrg. 80 (1989) 480–488.
[2] O. Coulaud, D. Funaro, O. Kavian, Laguerre spectral approximation of elliptic problems in exterior domains, Comput. Methods Appl. Mech. Engrg. 80 (1990) 451–458.
[3] V. Iranzo, A. Falqués, Some spectral approximations for differential equations in unbounded domains, Comput. Methods Appl. Mech. Engrg. 98 (1992) 105–126.
[4] Jie Shen, Stable and efficient spectral methods in unbounded domains using Laguerre functions, SIAM J. Numer. Anal. 38 (4) (2000) 1113–1133.
[5] Benyu Guo, Jie Shen, Laguerre–Galerkin method for nonlinear partial differential equations on a semi-infinite interval, Numer. Math. 86 (2000) 635–654.
[6] Lilian Wang, Benyu Guo, Stair Laguerre pseudospectral method for differential equations on the half line, Adv. Comput. Math. 25 (1–2) (2006) 305–322.
[7] Benyu Guo, Heping Ma, Composite Legendre–Laguerre approximation in unbounded domains, J. Comput. Math 19 (1) (2001) 101–112.
[8] Qingqu Zhuang, Chuanju Xu, A spectral element/Laguerre coupled method to the elliptic Helmholtz problem on the half line, Numer. Math. J. Chin. Univ. (Engl. Ser.) 15 (3) (2006) 193–208.
[9] Lilian Wang, Benyu Guo, Modified Laguerre pseudospectral method refined by multidomain Legendre pseudospectral approximation, J. Comput. Appl. Math. 190 (1–2) (2006) 304–324.
[10] M. Azaiez, Jie Shen, Chuanju Xu, Qingqu Zhuang, A Laguerre–Legendre spectral method for the Stokes problem in a semi-infinite channel, SIAM J. Numer. Anal. 47 (2008) 271–292.
[11] Jie Shen, Efficient spectral-Galerkin method. I: direct solvers of second-and fourth-order equations using Legendre polynomials, SIAM J. Sci. Comput. 15 (6) (1994) 1489–1505.
[12] Jie Shen, Lilian Wang, Laguerre and composite Legendre–Laguerre dual-Petrov–Galerkin methods for third-order equations, Discrete Contin. Dyn. Syst. Ser. B 6 (2006) 1381–1402.